

# An Efficient Solution to 6DOF Localization Using Unscented Kalman Filter for Planetary Rovers

Atsushi Sakai, Yuya Tamura and Yoji Kuroda  
Meiji University, Department of Mechanical Engineering,  
1-1-1 Higashimita, Tama-ku, Kawasaki, Kanagawa, Japan  
Email: asakai.amsl@gmail.com, {ce82037, ykuroda}@isc.meiji.ac.jp

**Abstract**—In this paper, we propose an efficient solution to 6 degrees of freedom (6DOF) localization using Unscented Kalman filter for planetary rovers. The solution is a technique augmented the Unscented Kalman filter for accurate 6DOF localization, named *Augmented Unscented Kalman Filter* (AUKF). The AUKF is designed to deal with problems which occur on other planets: wheel slip, visual odometry error, and gyro drift. To solve the problems, the AUKF estimates the slippage ratio in an augmented state vector, the accuracy of the visual odometry with the number of inliers among feature points, and sensor usefulness with Gyrodometry model. Experimental results of rover runs over rough terrain are presented, the effectiveness of the AUKF and its each component is shown.

**Index Terms**—6DOF localization, Unscented Kalman filter, slippage ratio estimation, planetary rover, visual odometry.

## I. INTRODUCTION

POSITION and attitude estimation is an important problem for planetary rover missions. For getting power effectively from solar panels and autonomous navigations for long distance, accurate position and attitude estimation is imperative. If the position and attitude estimation was more accurate, rover missions would be more efficient and effective.

Most of all surfaces of other planets are rough terrains. For rover navigations in the rough terrain, position and attitude estimation should consider 6 degrees of freedom (6DOF) consisted of rover's position ( $x, y, z$ ) and its attitude ( $roll, pitch, yaw$ ). Moreover, considering various problems in other planets (e.g., wheel slip on sandy surface, visual odometry error, and gyro drift) is also needed for accurate localization.

At the present day, the rover localization commonly uses Extended Kalman Filter (EKF) to integrate visual odometry, Inertial Measurement Unit (IMU), and wheel odometry [1][2]. The EKF is also used commonly for localization of general mobile robots [3]. There are, however, several problems to use the EKF for planetary rover localization. The first is that, in the EKF, a nonlinear model is approximated with Jacobian matrices. If the nonlinearity of the model is high, the accuracy of approximation becomes bad. In 6DOF localization, the motion model and the observation model have high nonlinearity, because these models have terms of coordinate transformation to all three coordinate axes. The second is that we must develop the expression for Jacobian matrices of the motion and the observation model. However,



Fig. 1. Micro6: our planetary rover testbed.

the derivation is difficult when the model is complicated like the rover's models.

The Particle filter is also well-used for ground mobile robot localization [4][5]. There are, however, also several problems to use the particle filter for planetary rover localization. Firstly, the estimation using the particle filter needs significant computational cost for 6DOF localization. Because, the 6DOF localization needs to compute the multidimensional probability. This is a serious problem in rover operations of which resources are limited. Secondly, a basic particle filter is easy to be influenced by pulsive noises. The pulsive noises occur frequently in rover missions, because the visual odometry is easy to induce the pulsive noises when being in low feature environments or not doing capture images correctly. The basic particle filter samples data randomly from an input source. If the pulsive noises occur, it may happen that there are no particles in the vicinity of the correct state, which is known as the particle deprivation problem [6].

In this paper, we propose to introduce Unscented Kalman filter (UKF) for the planetary rover localization to solve above problems. The method is based on the technique proposed by Julier and Uhlmann [7]. Afterward, the method is applied for various applications (e.g., Unmanned Aerial Vehicle localization, particle filter, and SLAM [8][9][10]). The UKF can estimate accurately high dimensions of probability because it can approximate an arbitrary nonlinear function. Besides, the expression for Jacobian matrices is not needed because the method estimates with information

of chosen sampling points. Therefore, the UKF is useful for the high dimension estimation like the planetary rover localization. Besides, computational cost of the UKF is very small about the same order of the EKF, and the UKF is robust to the pulsive noises because of using the Kalman filter framework. For these reasons, the UKF can be said that it is useful for the planetary rover localization.

The basic UKF is not enough for accurate localization. It is needed that wheel slip, visual odometry error, and gyro drift are solved. To solve the wheel slip problem, several researches have been done [11][12][13]. However, these studies can only detect that the wheel is slipped or estimate a slippage ratio using global information (e.g., GPS). For more practical rover localization, it is needed that the slippage ratio is estimated continuously without global information and prior information, and then the slippage ratio is used for localization. Pulsive noises of visual odometry, which occur once in a while, are also a serious problem. The noise may induce crucial localization error. It is important that the noise are dealt well to estimate accurately the rover position and attitude. The gyro drift is also an important problem for attitude estimation [16]. The error from the gyro drift accumulates, and then considerable attitude error may occur.

In this paper, for more accurate localization, we propose a 6DOF localization system named *Augmented Unscented Kalman Filter* (AUKF), which is augmented the UKF. The AUKF introduces three techniques as follows:

- 1) Slippage ratio estimation in an augmented state vector.
- 2) Visual odometry accuracy estimation with the number of inliers among feature points.
- 3) Introducing Gyrodometry model.

The first technique is that the slippage ratio is estimated in the augmented state vector. The second technique is that the accuracy of the visual odometry is estimated with the number of inliers among feature points, the rover motion is compensated with the accuracy. The third technique is to introduce the Gyrodometry Model [17]. Details of these techniques are described in following sections.

## II. MICRO6 SYSTEM

This section describes our planetary rover testbed. The planetary rover testbed is jointly developed at Meiji University, Chuo University, and Japan Aerospace eXploration Agency (JAXA), named *Micro6* (Fig. 1). It has 6 wheels connected by our unique suspension link system, named Huxus. The Micro6 has 3 sensors for position and attitude estimation: a stereo camera rig, an IMU, and wheel encoders on the 6 wheels. We use the stereo camera rig which is made up of Qcam for Notebooks Pro (QVX-13NS) made in Logicool co in this paper. The camera's interface is USB2.0, its resolution is VGA (640 × 480pix), and its baseline is 20cm. We use the IMU of NAV420CA-100 made in Crossbow co.

## III. UNSCENTED KALMAN FILTER

Unscented Transformation (UT) is a method for calculating the statistics of a random variable which undergoes a

nonlinear transformation. The UT built on the principle that it is easier to approximate a probability distribution of an arbitrary nonlinear function. The UT uses a small number of chosen test points, which are called *Sigma point*. The each sigma point is propagated through the nonlinear function, and then the mean and covariance are computed through the use of a weighted statistical linear regression process. The UT eliminates the cumbersome derivation and evaluation of Jacobian matrices. Besides, even if the model's nonlinearity is heavy, the accurate estimation is possible. It is known that the estimation of the mean and covariance is accurate to the second order of the Taylor series expansion of the nonlinear function. While, it is known that the EKF only calculates the posterior mean and covariance accurately to the first order with all higher order moments truncated [6]. Therefore, a filter based the UT is easier to implement and performs better than the EKF.

The UKF is a one of straightforward applications of the UT. The UKF estimation algorithm is organized as follows. The state vector is augmented with a control input and an observation as follows:

$$x_{t-1}^a = \begin{bmatrix} x_{t-1} \\ \mathbf{0} \\ \mathbf{0} \end{bmatrix} \quad (1)$$

Where  $x_{t-1}^a$  is the augmented vector of the state and  $x_{t-1}$  is the previous mean of the vehicle. Its covariance is also augmented.

$$P_{t-1}^a = \begin{bmatrix} P_{t-1} & \mathbf{0} & \mathbf{0} \\ \mathbf{0} & Q & \mathbf{0} \\ \mathbf{0} & \mathbf{0} & R \end{bmatrix} \quad (2)$$

Where,  $P_{t-1}^a$  is the augmented covariance,  $P_{t-1}$  is the previous covariance of the vehicle, and  $Q$  and  $R$  are an input noise covariance and a measurement noise covariance. The sigma points are extracted in Gaussian. In the general case, these sigma points are chosen at the mean and symmetrically along the main axes of the covariance. A symmetric set of sigma points  $\chi_{t-1}^{a[i]}$  is chosen according to the following rule:

$$\begin{aligned} \chi_{t-1}^{a[0]} &= x_{t-1}^a \\ \chi_{t-1}^{a[i]} &= x_{t-1}^a + (\sqrt{(N+\lambda)P_{t-1}^a})_i \quad i = 1, \dots, N \\ \chi_{t-1}^{a[i]} &= x_{t-1}^a - (\sqrt{(N+\lambda)P_{t-1}^a})_i \quad i = N+1, \dots, 2N \end{aligned} \quad (3)$$

Where,  $i$  is a index of sigma points,  $N$  is the dimension number of the augmented state vector,  $\lambda$  is computed by  $\lambda = \alpha^2(N + \kappa) - N$ , with  $\alpha$  and  $\kappa$  are scaling parameters that determine how far the sigma points are spread from the mean  $x_{t-1}^{a[0]}$ . In this paper,  $\alpha$  is set to  $10^{-3}$ ,  $\kappa$  is set to 0. Each sigma point is propagated through the nonlinear function, thereby probing how the nonlinear function changes the shape of Gaussian. The set of sigma points  $\chi_{t-1}^{a[i]}$  is transformed by the nonlinear motion model  $\mathbf{f}$  using the current input  $u_t$  and the control noise component  $\chi_t^{u[i]}$  as follows:

$$\bar{\chi}_t^{[i]} = \mathbf{f}(u_t + \chi_t^{u[i]}, \chi_{t-1}^{a[i]}) \quad (4)$$

Here  $\bar{\chi}_t^{[i]}$  is the transformed sigma points of the state vector. The parameters,  $x_{t|t-1}$  and  $P_{t|t-1}$ , of the resulting Gaussian are computed by a linear weighed regression of the transformed sigma points  $\bar{\chi}_t^{[i]}$  as follows:

$$x_{t|t-1} = \sum_{i=0}^{2N} \omega_g^{[i]} \bar{\chi}_t^{[i]} \quad (5)$$

$$P_{t|t-1} = \sum_{i=0}^{2N} \omega_c^{[i]} (\bar{\chi}_t^{[i]} - x_{t|t-1})(\bar{\chi}_t^{[i]} - x_{t|t-1})^T \quad (6)$$

Here  $\omega_g^{[i]}$  are weighs used when the mean is computed,  $\omega_c^{[i]}$  are weighs used when the covariance of Gaussian is recovered. These wights are calculated as the following rule:

$$\begin{aligned} \omega_g^{(0)} &= \frac{\lambda}{N + \lambda} \\ \omega_c^{(0)} &= \frac{\lambda}{N + \lambda} + (1 - \alpha + \beta) \\ \omega_g^{(i)} &= \omega_c^{(i)} = \frac{1}{2(N + \lambda)} \quad i = 1, \dots, 2N \end{aligned} \quad (7)$$

Where,  $\beta$  is chosen to incorporate higher order knowledge about the distribution underlying Gaussian representation. In this paper, the distribution is supposed being an exact Gaussian, we set the parameter  $\beta = 2$  as knowing the optimal value. Sigma points of the observation  $\bar{N}_t^{[i]}$  are propagated through the nonlinear observation model  $\mathbf{h}$  using the localization component of each sigma point  $\bar{\chi}_t^{[i]}$  and the observation noise component  $\chi_t^{z[i]}$  of each sigma point.

$$\bar{N}_t^{[i]} = \mathbf{h}(\bar{\chi}_t) + \chi_t^{z[i]} \quad (8)$$

A prediction of observation  $\hat{n}_t$  and its covariance  $S_t$  are computed by following equations:

$$\hat{n}_t = \sum_{i=0}^{2N} \omega_g^{[i]} \bar{N}_t^{[i]} \quad (9)$$

$$S_t = \sum_{i=0}^{2N} \omega_c^{[i]} (\bar{N}_t^{[i]} - \hat{n}_t)(\bar{N}_t^{[i]} - \hat{n}_t)^T \quad (10)$$

The cross-covariance between robot localization and observation  $\Sigma_t^{x,n}$  is determined by following Eq. (11):

$$\Sigma_t^{x,n} = \sum_{i=0}^{2N} \omega_c^{[i]} (\bar{\chi}_t^{[i]} - x_{t|t-1})(\bar{N}_t^{[i]} - \hat{n}_t)^T \quad (11)$$

The Kalman gain  $K_t$  is computed by following Eq. (12):

$$K_t = \Sigma_t^{x,n} (S_t)^{-1} \quad (12)$$

Finally, the mean  $x_t$  and the covariance  $P_t$  of the probabilistic distribution of the localization are calculated by following equations:

$$x_t = x_{t|t-1} + K_t(z_t - \hat{n}_t) \quad (13)$$

$$P_t = P_{t|t-1} - K_t S_t (K_t)^T \quad (14)$$

#### IV. AUGMENTED UNSCENTED KALMAN FILTER

In this paper, we propose a technique to augment the UKF for accurate position and attitude estimation, named Augmented Unscented Kalman Filter (AUKF). The AUKF aims to deal with the problems which are easy to occur on surfaces of other planets (e.g, wheel slip, visual odometry error, and gyro drift). We introduced the three techniques to solve these problems.

##### A. Slippage ratio estimation

The wheel slip is a primary problem on rover navigation. In this paper, we propose to estimate the slippage ratio to be token in the state vector. The slippage ratio  $i$  at the time  $t$  is determined as following:

$$i_t = 1 - \frac{v_{true,t}}{v_{wo,t}} \quad (15)$$

where  $v_{wo,t}$  is a forward velocity of the wheel odometry, and  $v_{true,t}$  is a true forward velocity (no slip). We use a observation of the visual odometry as the true forward velocity. However, the slippage ratio which is calculated directly with the Eq. (15) is noisy, because the observation of the visual odometry is instability. The localization may be insecurity using the slippage ratio directly. Moreover, if the slippage ratio is used for localization, it should be estimated as a function of exploration environments and running speeds. Because the ratio changes on running environments and traveling speed.

In AUKF, the state vector is augmented by the slippage ratio:

$$\mathbf{x}_t = [x_t, y_t, z_t, roll_t, pitch_t, yaw_t, i_t]^T \quad (16)$$

It is estimated same as for other state components. Eq. (15) is modeled as the observation model, and the slippage is updated with both observations of the visual odometry and the wheel odometry. And then, the estimated slippage ratio is used for the localization. In AUKF, the forward velocity component of input vector is determined as follows:

$$u_{fv,t} = (1 - i_t)v_{wo,t} \quad (17)$$

where,  $u_{fv,t}$  is the forward velocity component of input vector at the time  $t$ . Information of visual odometry is used in the form of the slippage ratio for position and attitude estimation. Furthermore, slippage ratios can be estimated on several running environments and several traveling speeds due to initializing the covariance of the AUKF.

##### B. Assuming plane motion with the number of inliers among feature points

The visual odometry is not always accurate. For example, the visual odometry is often unable to function when feature points are not detected because of rapid image alterations or being in low feature environments. In these situations, the visual odometry becomes instability, may have catastrophic error (e.g., pulsive noise). Especially, errors of the vertical and lateral directions from the moving direction are significant problems because rovers usually lack another sensor which can get information regarding the error.

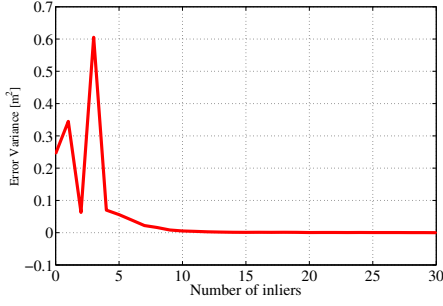


Fig. 2. Relationship between the number of inliers and error variance at an experiment.

In order to solve the problem, we propose to evaluate the accuracy of the visual odometry using the number of inliers among feature points. The number of inliers can be obtained using the framework of RANdom Sample Consensus (RANSAC) and 3-point algorithm in motion estimation process [14][15]. First, a hypothesis of the motion parameter is generated from a sample of the 3 set of data points randomly selected from all data points. After that, all feature points observed before movement are reprojected into the current image frame using the hypothesis. Next, we calculate the reprojection error to each point. If the reprojection error is smaller than a threshold, the data is regarded as inliers. Final, we count the number of inliers.

We executed an experiment for showing the relationship between the number of inliers and the accuracy of visual odometry. In the experiment, we moved the stereo camera rig by 10 cm, and the results of estimation and the number of inliers are measured. Fig. 2 shows the relationship between the number of inliers and the error variance at the experiment. The result shows that there is a correlation between the number of inliers and the estimation error. When the number of the inliers is high, the accuracy of visual odometry is good, while when the inlier number is low, the accuracy is bad.

In this paper, we propose to assume the rover motion with the number of the inliers for preventing the influence from the visual odometry error. If the accuracy is high, the input of visual odometry is used as-is, or if the accuracy is low, the rover motion is assumed to be plane motion. The plane motion is that the lateral motion  $dy_{vo}$  and the vertical motion  $dz_{vo}$  are nothing. Because of it, the lateral and vertical estimation error is prevented. In AUKF, the components of input are determined with the following rule:

```

if  $N_{inliers} > N_{th}$ 
     $dy = dy_{vo}, dz = dz_{vo}$ 
else
     $dy = dz = 0$ 
endif

```

Here,  $N_{inliers}$  is the number of inliers,  $N_{th}$  is the threshold of the number of inliers.



Fig. 3. Experimental fields: Field A is a slow ascent field (the left picture), Field B has an undulations and several blockades (the right picture). The red solid lines in the both pictures are the rover trajectories in the experiments.

### C. Gyrodometry model for planetary rover

The gyro drift is also an important problem in rover localization [9]. The drift brings on an error bias; the bias will cause the localization error. When the rover is moving straight, the  $dyaw$  component of the wheel odometry are accurate than the IMU, because the data from the IMU involves the gyro bias. While, when the wheel slip occurs, the gyro should be used for localization because slip error is often bigger than the gyro bias error.

In the AUKF, the  $dyaw$  component is selected with Gyrodometry model [17]. Gyrodometry model is an effective method for combining measurements from a gyro with measurements from wheel encoders. The method can anticipate a non-systematic odometry and gyro error (e.g., slip, bump, and gyro bias). In Gyrodometry model, the  $dyaw$  component is selected with the following rule:

```

 $\Delta_t = |dyaw_{(gyro,t)} - dyaw_{(wo,t)}|$ 
if  $\Delta_t > \Delta_{theres}$ 
     $dyaw = dyaw_{(gyro,t)}$ 
else
     $dyaw = dyaw_{(wo,t)}$ 
endif

```

Here,  $\Delta_t$  is the discrepancy between the  $dyaw$  element of the odometry and the gyro at the time  $t$ , and  $\Delta_{theres}$  is the threshold value of the discrepancy.

## V. EXPERIMENTAL RESULTS

In this section, we present experimental results using the Micro6 aimed at assessing the overall effectiveness of the AUKF. We performed three runs on the outdoor rough terrain (Fig. 3). Details of the three runs were as follows:

- Run 1: The rover ran at a constant speed along a straight-line path in Field A (the left picture of Fig. 3).
- Run 2: The rover ran with stop-start movements along a straight-line path in Field A
- Run 3: The rover ran along a closed-loop path in Field B (the right picture of Fig. 3), in which the rover encountered undulations and several blockades, then the rover K-turned to escape these impediments.

Using data sets gotten in these experiments, we present the effectiveness of our methods in after sections.

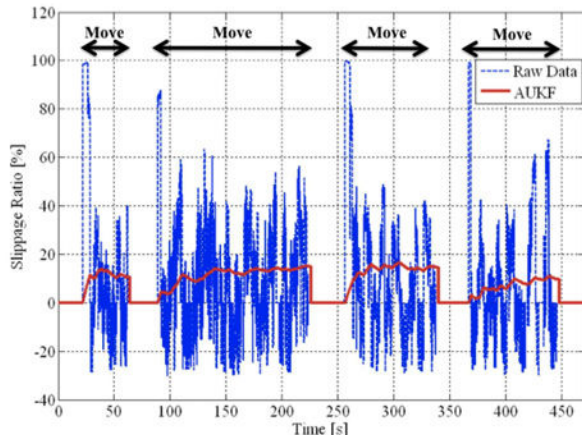


Fig. 4. Slippage ratio estimation (Run 2).

TABLE I  
RESULT OF GYRODOMETRY MODEL (RUN 1).

	Mean Absolute Error [rad/s]
Inertial Measurement Unit	0.017921
Wheel Odometry	0.017533
Gyrodometry Model	0.015717

#### A. Result of Slippage Estimation

We demonstrate the effectiveness and impact of the slippage ratio estimation. Fig. 4 shows the result of the slippage ratio estimation at Run 2. This result shows that the slippage ratio calculated directly from the raw data is instability. If the noisy data is used as-is, the localization may be instability. While, the slippage ratio estimated by our technique was estimated stably with considering the other state components. Moreover, in the experiment, the AUKF judged whether the rover was stop or move with input triggers, then the covariance of the AUKF was initialized when the rover was stop. As the results, the slippage ratio was estimated for the each move period. Because of using triggers, it will become possible that the appropriate slippage ratio is estimated in the environment which has parts of different slippage ratio and when the rover runs on the different speeds.

#### B. Result of Gyrodometry Model

We show the effectiveness of introducing Gyrodometry model. Table I shows the mean absolute error of the experimental results at Run 1. In the experiment, the true  $dyaw$  value to calculate the error was taken by a fiber optical gyro (FOG) (the FOG is not used for the rover localization). The FOG measurement is very accurate (the angle drift is under  $\pm 0.5deg/h$ ). Table I indicates that the mean absolute error with Gyrodometry model is the smallest of the all methods. Gyrodometry model reduced the mean absolute errors by almost 12% from the result only using the IMU and by almost 10% from the result only using the wheel odometry. Therefore, it was shown that the  $dyaw$  component became more accurate in virtue of introducing Gyrodometry model.

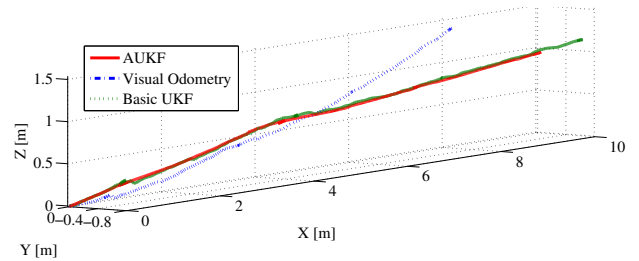


Fig. 5. Result of 6DOF localization (Run 1).

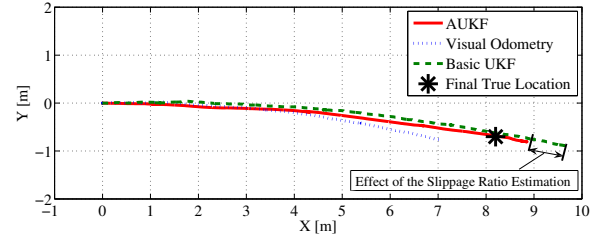


Fig. 6. Result of localization on the x-y surface (Run 1).

#### C. Results of 6DOF localization

In this section, we show the localization results of the experiments. Fig. 5 shows the result of 6DOF localization at Run 1. Fig. 5 has the three trajectories of the visual odometry, a basic UKF, and the AUKF. The basic UKF estimated only the rover position ( $x, y, z$ ) and the attitude ( $roll, pitch, yaw$ ). The parameters used the AUKF and the basic UKF in common were same. Fig. 6 shows the result of localization on the x-y surface at Run 1. The final true location in the figure indicates the actual point where the rover stops. The figure indicates that the end of the trajectory using only the visual odometry stays off the stop point. The end of the trajectory using the basic UKF is near the stop point, but it has the error of the direction of movement because of the wheel slip. The end of the AUKF's trajectory is the nearest of all trajectories to the stop point. The arrow in the figure shows the effect of the slippage estimation.

Fig. 7 shows the result of 6DOF localization at Run 3. Fig. 7 has the three trajectories as same Fig. 5. The figure indicates that the trajectory of the visual odometry could not return to the start point (coordinate origin). The trajectory of the basic UKF is more accurate than the visual odometry, but the error along the z axis remained. On the other hand, the AUKF reduce the error along the z axis due to the assuming plane motion with the number of inliers. Fig. 8 show the results of localization on the x-y surface at Run 3. This figure also indicates the K-turn points. The terminating point of the AUKF's trajectory is the nearest of all trajectories from the start point.

Table II shows the final position errors and the error ratios to the moving distance at Run 1 and Run 3. The errors are Euclidean distances between the estimated final point and the actual final point on the x-y surface. The rover moved about  $8.5m$  at Run 1, and about  $18.8m$  at Run 3. Table II shows

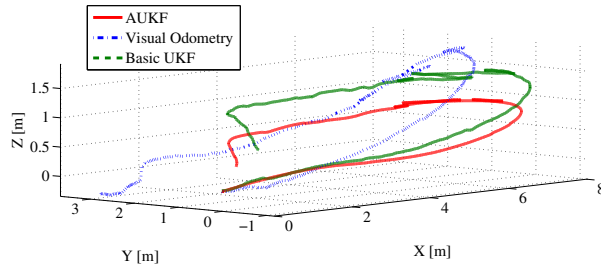


Fig. 7. Result of 6DOF localization (Run 3).

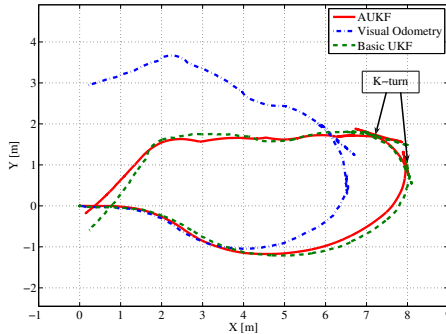


Fig. 8. Result of localization on the x-y surface (Run 3).

that the error of AUKF is the smallest of the all methods in both runs. Because of using the AUKF, the position error decreased over 50% from the other methods at Run 1, over 80% from using the visual odometry at Run 3, and 50% from using the basic UKF at Run 3.

Accordingly, it was shown the effectiveness of the AUKF from these experimental results.

## VI. CONCLUSION

In this paper, we proposed an efficient solution to the 6 DOF localization for planetary rovers. To solve problems of conventional filters, we proposed to introduce the Unscented Kalman Filter for planetary rover localization. Moreover, we proposed a technique augmented the Unscented Kalman filter, named Augmented Unscented Kalman Filter (AUKF). Experimental results of rover runs over rough terrain were presented, the effectiveness of the AUKF and its each component was shown.

## REFERENCES

- [1] K.S. Ali, C.A. Vanelli, J.J. Biesiadecki, M.W. Maimone, Y. Cheng, M.S. Martin, and J.W. Alexander, "Attitude and position estimation on the Mars exploration rovers", in Proc. IEEE Conf. Syst., Man, Cybern., The Big Island, HI, pp. 20-27, Oct. 2005.
- [2] K. Konolige, M. Agrawal, and J. Sola. "Large-scale visual odometry for rough terrain.", In Proceedings of the International Symposium on Research in Robotics, Hiroshima, Japan, November 26-29 2007.
- [3] G. Welch and G. Bishop. "An Introduction to the Kalman Filter", ACM SIGGRAPH, 2001.
- [4] D. Fox. "Adapting the Sample Size in Particle Filters through KLD-Sampling", J. Robotics Research, vol. 22, to be published, 2003.

TABLE II  
RESULT OF LOCALIZATION (RUN 1 AND RUN 3).

	Final Position Error [m]	Error Ratio [%]
Visual Odometry (Run 1)	1.2374	14.6
Basic UKF (Run 1)	0.9779	11.5
AUKF (Run 1)	0.5238	6.1
Visual Odometry (Run 3)	2.9485	15.7
Basic UKF (Run 3)	0.9779	5.2
AUKF (Run 3)	0.4837	2.6

- [5] Sebastian Thrun, Dieter Fox, Wolfram Burgard, and Frank Dellaert. "Robust Monte Carlo Localization for Mobile Robots.", Artificial Intelligence, 128(1-2):99-141, 2001.
- [6] S. Thrun W. Burgard, D. Fox, "Probabilistic Robotics.", MIT Press, 2005.
- [7] Julier and J. K. Uhlmann, "General method for approximating non-linear transformations of probability distributions", Robotics Research Group Department of Engineering Science, University of Oxford 1996.
- [8] R. van der Merwe, "Sigma-Point Kalman Filters for Probabilistic Inference in Dynamic State-Space Models.", PhD thesis, OGI School of Science & Engineering at Oregon Health & Science University, Portland, OR, April 2004.
- [9] R. Merwe, A. Doucet, N. Freitas and E. Wan, "The Unscented Particle Filter", Technical Report CUED/F-INFENG/TR 380, Cambridge University Engineering Department, 2000.
- [10] C.Kim, R.Sakthivel, and W.K.Chung, "Unscented FastSLAM: A robust algorithm for the simultaneous localization and mapping problem", in Proc. IEEE Int. Conf. Robot. Autom., pp. 2439-2445, 2007.
- [11] Helmick, D., Roumeliotis, S., Cheng, Y., Clouse, D., Bajracharya, M., Matthies, L., "Slip compensation for a Mars rover", IROS, 2005.
- [12] D. Lindgren, T. Hague, P. Probert Smith, and J. Marchant, "Relating torque and slip in an odometric model for an autonomous agricultural vehicle", Auton. Robots, vol. 13, no. 1, pp. 73-86, Jul. 2002.
- [13] L. Ojeda, D. Cruz, G. Reina, J. Borenstein, "Current-based slippage detection and odometry correction for mobile robots and planetary rovers", IEEE Transactions on Robotics 22 (2), 366-378, 2006.
- [14] M.W. Maimone, Y. Cheng, L. Matthies, "Two Years of Visual Odometry on the Mars Exploration Rovers", Journal of Field Robotics, Volume 24 number 3, special issue on Space Robotics, Mar. 2007.
- [15] K. Ni, and F. Dellaert, "Stereo tracking and three-point/one point algorithms - a robust approach in visual odometry", In International Conference on Image Processing, 2006.
- [16] Y. Fuke and E. Krotkov. "Dead reckoning for a lunar rover on uneven terrain", In Proceedings of the 1996 IEEE International Conference on Robotics and Automation, pages 411-416, 1996.
- [17] Borenstein, J., Feng, L. "Gyrodometry: A New Method for Combining Data from Gyros and Odometry in Mobile Robots", Proceedings 1996 IEEE International Conference on Robotics and Automation, Vol. 1, pp 423-428, 1996.
- [18] D.M. Helmick, Y. Cheng, S.I. Roumeliotis, D. Clouse, and L. Matthies, "Path following using visual odometry for a Mars rover in high-slip environments", in Proc. IEEE Aerospace Conf., Big Sky, MT, 2004.
- [19] Biesiadecki, J. J., and M. W. Maimone, "The Mars Exploration Rover Surface Mobility Flight Software: Driving Ambition", IEEE Aerospace Conference, Big Sky, Montana, USA, Vol. 5, Mar. 2005.
- [20] E. T. Baumgartner, H. Aghazarian, and A. Trebi-Ollennu, "Rover localization results for the FIDO rover," in Proc. SPIE Conf. Sensor Fusion and Decentralized Control in Autonomous Robotic Systems IV, vol. 4571, Newton, MA, Oct 2001.
- [21] Li, R., K. Di, L.H. Matthies, R.E. Arvidson, W.M. Folkner and B.A. Archinal. "Rover Localization and Landing Site Mapping Technology for 2003 Mars Exploration Rover Mission", Journal of Photogrammetric Engineering and Remote Sensing, Vol.70(1): 77-90, 2003.
- [22] D. Helmick, A. Angelova, and L. Matthies, "Terrain Adaptive Navigation for Planetary Rovers", Journal of Field Robotics 26(4), 391-410, 2009
- [23] D. Nister, O. Naroditsky, and J. Bergen, "Visual Odometry", Proc. IEEE Computer Society Conference on Computer Vision and Pattern Recognition, Volume 1, 2004, pp.652-659.